



OPEN ACCESS

EDITED BY

Marcello Natalicchio,
University of Turin, Italy

REVIEWED BY

Tapan Chakraborty,
Indian Statistical Institute, India
Douaa Fathy,
Minia University, Egypt

*CORRESPONDENCE

Lin Jiang,
✉ jianglin01@petrochina.com.cn

RECEIVED 05 March 2025

ACCEPTED 28 July 2025

PUBLISHED 29 August 2025

CITATION

Feng Y, Jiang L, Jiang H, Gao Y, Zhao W,
Zhang T and Hu Y (2025) Sedimentary model
controlled by alternating dry-wet climatic
cycles environment of Yanchang Formation
and exploration significance in upper Triassic,
Ordos basin.

Front. Earth Sci. 13:1587896.

doi: 10.3389/feart.2025.1587896

COPYRIGHT

© 2025 Feng, Jiang, Jiang, Gao, Zhao, Zhang
and Hu. This is an open-access article
distributed under the terms of the [Creative
Commons Attribution License \(CC BY\)](#). The
use, distribution or reproduction in other
forums is permitted, provided the original
author(s) and the copyright owner(s) are
credited and that the original publication in
this journal is cited, in accordance with
accepted academic practice. No use,
distribution or reproduction is permitted
which does not comply with these terms.

Sedimentary model controlled by alternating dry-wet climatic cycles environment of Yanchang Formation and exploration significance in upper Triassic, Ordos basin

Yingqi Feng^{1,2}, Lin Jiang^{1,2*}, Hua Jiang^{1,2}, Yang Gao^{2,3},
Wen Zhao^{1,2}, Tongxi Zhang³ and Yao Hu^{2,3}

¹PetroChina Research Institute of Petroleum Exploration and Development, Beijing, China, ²CNPC Key Laboratory of Basin Structure and Hydrocarbon Accumulation, Beijing, China, ³College of Geosciences, China University of Petroleum (Beijing), Beijing, China

The Ordos Basin, one of China's most significant onshore oil and gas basins, hosts the Triassic Yanchang Formation, renowned for its multi-layered oil production and three-dimensional distribution of diverse hydrocarbon resources. The formation's abundant crude oil reserves, coupled with the stratified distribution of shale oil, tight oil, and conventional oil, have garnered substantial attention from researchers globally. Understanding the distribution patterns and controlling factors of these reservoirs is crucial for optimizing exploration and development strategies. This study provides a comprehensive analysis of the sedimentary facies within the Yanchang Formation, elucidating the interplay between sedimentary sequences and environmental-climatic changes. It challenges the traditional view that lake-level fluctuations predominantly control reservoir sand body distribution, proposing instead a new sedimentary model driven by the combined effects of tectonic activity and alternating dry-wet climatic conditions. Our findings reveal that the Yanchang Formation's climate exhibited a tripartite division, with abrupt climatic fluctuations likely influenced by major tectonic events such as those related to the Qinling orogeny such as the Qinling orogeny. The middle Triassic (Chang 10~Chang 8) and late Triassic (Chang 3~Chang 1) stages were characterized by arid conditions. During these periods, the eastern basin, with its gentle topography and limited catchment areas, was dominated by flood-driven sedimentation events. In contrast, the steeper western region developed extensive braided river deltas. The middle stage (Chang 7~Chang 4 + 5), influenced by the Carnian Pluvial Episode (CPE), experienced a humid climate, fostering fluvial, deltaic, lacustrine and gravity flow deposits and the development of high-quality source rocks. Additionally, this study identifies and systematically analyzes sedimentary facies unique to arid environments during low lake-level stages: the fluvial fan system. We define its developmental conditions, distribution patterns, and sedimentary sequence variations in response to climatic changes. This discovery challenges the conventional view that the Yanchang Formation is dominated by shallow-water delta deposits, offering new insights into the sedimentary theory of

continental basins and providing valuable guidance for future oil and gas exploration.

KEYWORDS

Ordos basin, late triassic, yanchang formation, paleoclimate, major geological events, sedimentary facies, delta, fluvial fan

1 Introduction

The Ordos Basin is one of the most important onshore oil and gas basins in China, and the Yanchang Formation of the Middle and Upper Triassic Series represents the primary oil-bearing interval with relatively complete stratigraphic development. Previous studies have only focused on the sedimentary systems of the lower Yanchang Formation (Deng et al., 2009; Guo et al., 2019; Li et al., 2019). However, detailed studies on the sedimentary facies and evolution of the entire Yanchang Formation remains limited. Earlier studies suggested that the Yanchang Formation was characterized by a humid climate, with delta facies widely distributed (Deng et al., 2008; Fu et al., 2005; Wu et al., 2004). In recent years, based on detailed observations, descriptions, and laboratory analyses of paleosols, paleoclimate indicators, and extensive outcrop data, Li X. et al. (2023) proposed that the climate of the Yanchang Formation alternated between dry and wet conditions, indicating that the entire formation was not uniformly humid. With the deepening of research, the impact of abrupt climatic events on the Yanchang Formation cannot be overlooked. The Carnian Pluvial Episode (CPE), occurring approximately 234–232 Ma, represents one of the most significant climatic events of the Mesozoic. It has garnered initial attention from numerous scientists due to the deposition of black shales in the shelves of the Paleo-Tethys and Neo-Tethys Oceans (Gao et al., 2025; Hu et al., 2025; Schlager and Schöllnberger, 1974; Simms and Ruffell, 1989; Xie et al., 2024). In addition, significant changes in sedimentary environments occurred during this period, such as the transition from sabkha and salt lake deposits across continental Europe to river-delta deposits in the northwestern Tethys Sea (Kozur and Bachmann, 2010). The global climatic environment underwent substantial changes before and after the CPE event. Prior to the CPE event, the global climate experienced prolonged aridity. During the event, a period of intense rainfall lasting approximately 1 Ma occurred, followed by a return to arid conditions (Nakada et al., 2014). This pattern is consistent with the paleoclimatic changes observed in the Yanchang Formation (Li et al., 2023b). This characteristic not only corresponds to the Carnian Pluvial Episode but also reflects the tectonic-sedimentary evolution of the lake basin, which transitioned from an initial restricted phase under arid conditions to a middle phase characterized by peak lake expansion, followed by a late phase of gradual lake retreat and eventual disappearance. Tectonic activity drove the expansion and subsequent contraction of the lake basin, while climatic cycles exerted a significant influence on the depositional processes of the Yanchang Formation. Furthermore, other geological events, such as volcanic eruptions and gravity flow events, contributed to the sedimentary characteristics and spatial distribution of the Yanchang Formation. These factors collectively controlled and shaped the present-day sedimentary architecture (Li et al., 2023a).

Climatic conditions exert significant control over sedimentary processes in continental lacustrine basins, with markedly distinct terrigenous clastic depositional patterns developing under arid versus humid environments (Nichols and Hirst, 1998; Pan et al., 2012; Zavala and Freije, 2001). Recently, the extensive fan-like river systems have been termed fluvial fans or distributive fluvial systems (Hartley et al., 2010; North and Warwick, 2007; Weissmann et al., 2010; Zhang et al., 2020a). These systems are characterized by floodplain depositional environments formed by the repeated avulsion of meandering rivers from their source areas (Cain and Mountney, 2009; Li, 2018a; North and Warwick, 2007). Fluvial fans represent terrestrial sedimentary systems, whereas deltas constitute the subaqueous continuation of fluvial fans, often leading to confusion between the two. The identification of the lake shoreline is critical for distinguishing deltas from fluvial fans.

Based on previous studies, sedimentary characteristics were analyzed using typical single-well and connected-well profiles. The sedimentary facies of each interval within the Yanchang Formation were redefined, and the distribution patterns of sedimentary facies under the combined influence of alternating dry-wet climatic conditions and tectonic activity were determined. Furthermore, a sedimentary evolution model was established.

2 Geological settings

The Ordos Basin, located in the western part of the North China Plate, is bounded by the Yinshan Mountain Range to the north, the Qinling Mountain Range to the south, the Luliang Mountain system to the east, and the Helan-Liupan Mountain system to the west, covering an extensive area of approximately $37 \times 10^4 \text{ km}^2$. During the Middle and Late Triassic, the basin experienced uplift due to the Indosinian Movement. The present-day topography of the Ordos Basin reveals a broad and gentle eastern flank with low terrain, contrasting with a steep and narrow western flank characterized by higher elevation. The central part of the basin exhibits relatively gentle topography, with tectonic activity primarily dominated by regional uplift and subsidence, resulting in the formation of a large, east-west asymmetric synclinal basin (Liu et al., 2011; Zhang et al., 2019). Based on prominent stratigraphic features, gravity, magnetic, and electrical characteristics, as well as the unique structural attributes of the basement top surface, the basin can be divided into several structural units: the Tianhuan Depression, the Western Margin Thrust Belt, the Northern Shaanxi Slope, the Western Shanxi Flexural Belt, and the Weibei Uplift (Liu et al., 2007; Lu et al., 2008) (Figure 1C).

During the Triassic, the Ordos Basin was situated along the coast of the Tethys Domain near 30° N latitude (Carroll et al., 2010) (Figure 1A). Influenced by the collision and convergence of the South China Plate and the mid-North China Block, the

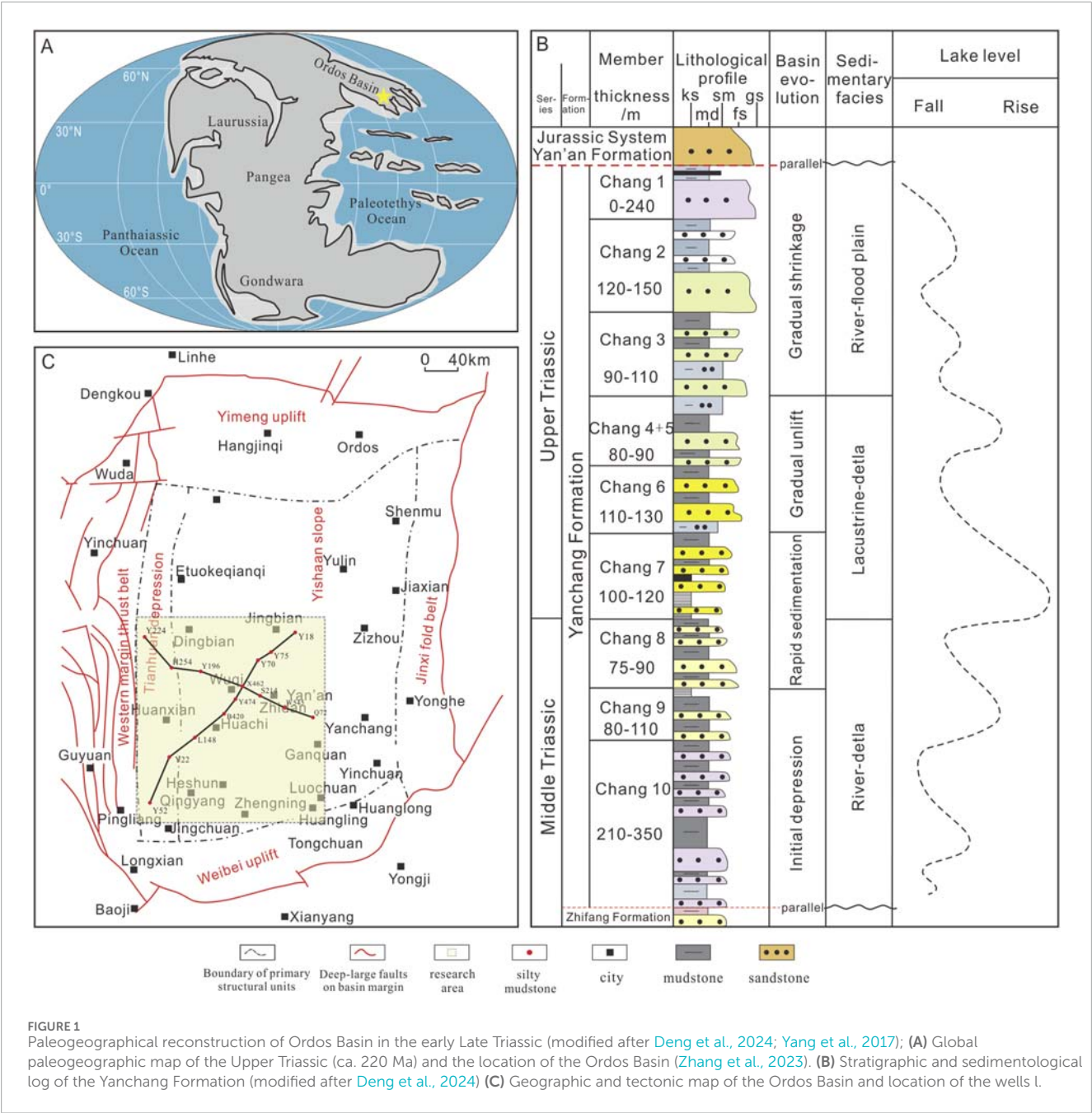


FIGURE 1 Paleogeographical reconstruction of Ordos Basin in the early Late Triassic (modified after [Deng et al., 2024](#); [Yang et al., 2017](#)); **(A)** Global paleogeographic map of the Upper Triassic (ca. 220 Ma) and the location of the Ordos Basin ([Zhang et al., 2023](#)). **(B)** Stratigraphic and sedimentological log of the Yanchang Formation (modified after [Deng et al., 2024](#)) **(C)** Geographic and tectonic map of the Ordos Basin and location of the wells l.

basin underwent significant subsidence, leading to extensive lake transgression. The Yanchang Formation was deposited during this period, with a sedimentary thickness ranging from 1000 to 1300 m. The formation is divided into 10 members (Chang 10 ~ Chang 1) from bottom to top ([Deng et al., 2024](#)). The early stage (Chang 10 ~ Chang 8) represents the initial development phase of the Yanchang Formation and the lake basin, during which the Indosinian Movement was relatively weak. The middle stage (Chang 7 ~ Chang 4 + 5) was marked by intensified tectonic activity, with the lake basin reaching its maximum extent during the Chang 7 Stage. This period corresponds to the peak maximum lake expansion phase and the most prolific development of Mesozoic source rocks ([Liu et al., 2022](#)), making it a key target for shale oil exploration

and development ([Lu et al., 2022](#); [Pang et al., 2022](#)). Subsequently, the lake basin gradually shrank. The late stage (Chang 3 ~ Chang 1) witnessed further contraction and eventual disappearance of the lake basin. Concurrently, the basin experienced uplift and reworking due to the Indosinian Movement, resulting in unconformities at the top and base of the Yanchang Formation, with significant erosion observed at the top ([Figure 1B](#)).

During the Triassic, the Ordos Basin was situated within the arid climatic zone (45°S ~ 50°N), which encompassed regions such as the Gondwana continent and North China of the Paleotethys ([Tusken et al., 2014](#)). Paleontological and paleosedimentary evidence generally indicates arid climatic conditions during this period. However, the basin's proximity to the ancient Rauya

continent to the east, as well as its location between the “Tethys Sea” to the south and the “Mongol-Okhotsk Ocean” to the north (Tusken et al., 2014), facilitated increased atmospheric precipitation due to its closeness to oceans and mountain ranges, resulting in localized humid conditions (Parrish, 1993; Parrish and Peterson, 1988). Concurrently, intense Indosinian tectonic activity in the southern part of the basin led to the uplift of the basin margin, forming the Qinling Orogenic Belt (Yang et al., 2017). Large-scale volcanic eruptions during this period increased atmospheric CO₂ concentrations, enhancing the global greenhouse effect. Combined with the influence of the Triassic monsoon, these factors contributed to elevated rainfall, creating favorable conditions for rapid basin subsidence during the middle Yanchang Formation and the development of localized humid climatic environments.

3 Methods

Based on data from over 500 wells in the study area, the sedimentary environment was comprehensively analyzed by integrating lithology, core data, and log facies characteristics. Initially, typical wells from different structural positions were selected to systematically discriminate and classify the sedimentary facies of the Chang 10 to Chang 1 strata. Key sedimentological facies characteristics were identified during this process. Subsequently, two representative well-tied sedimentary profiles were chosen to define the sedimentary facies and evolutionary patterns of the Yanchang Formation in the study area. The areal distribution of sedimentary facies was investigated, and a longitudinal sedimentary facies evolution model through time for the entire Yanchang Formation was established.

4 Results

4.1 Sedimentary facies types and characteristics

Eighteen wells in the study area were selected as representative examples. Through the analysis of sedimentological features, including core color, lithology, sedimentary structures, and log facies characteristics (Table 1), sedimentary facies types such as delta, fluvial fan, and lacustrine systems were identified. Additionally, the log facies characteristics of different sedimentary facies systems were systematically summarized (Table 2). Fluvial fan deposits are frequently misidentified as deltaic systems, particularly when compared to shallow-water deltas developed in humid environments. Unlike deltas that form through sediment dispersion at river-lake interfaces, fluvial fans originate through channel migration, avulsion, and vertical stacking of deposits over time within seasonally influenced basins. These systems typically occur in hydrologically closed basins where lake levels fluctuate dramatically between wet and dry seasons - accumulating water during precipitation events but experiencing rapid evaporation or complete desiccation during arid periods, as exemplified by Bolivia's Uyuni Salt Lake which remains dry except during seasonal rains. Consequently, fluvial fan systems like the Colorado River fan lack characteristic deltaic features such as subaqueous distributary

channels or mouth bars (Li, 2018b). In contrast, deltas represent fan-shaped sedimentary bodies that develop when terrestrial rivers discharge into standing water bodies, with their formation being fundamentally controlled by the interaction between fluvial inputs and lacustrine/marine processes. Deltaic systems are distinguished by both the buoyancy and flow diversion effects of receiving water bodies at river mouths, as well as subsequent reworking by wave and tidal processes that significantly modify the original fluvial.

4.1.1 Fluvial fans facies systems

Fluvial fans are fan-shaped sedimentary systems formed by the repeated avulsion of terrestrial rivers, primarily developing under all climatic condition and also common in areas with dryland climate (Hartley et al., 2010). These fans are characterized by flat depositional topography, distant sediment sources, and large radii. Based on the types of channels developed on the fan surface, fluvial fans can be classified into braided river fans and meandering river fans, collectively referred to as fluvial fans (Galloway et al., 1996; Stanistreet and McCarthy, 1993).

Sedimentary facies interpretation based on core samples, well logs characteristics reveals that the most significant distinction between fluvial fans and typical meandering river deposits. Sandstones often exhibit abrupt contacts with overlying and underlying mudstones, as observed in wells G55 and Y18 (Figure 2). This indicates sudden lake-level rise followed by rapid retreat and rapid sediment deposition, reflecting the intermittent activity of fluvial system. These features suggest that fluvial deposition was dominated by episodic flooding under arid paleoclimatic conditions and gentle paleotopography (Hartley et al., 2010).













The main sedimentary units of fluvial fans include channel deposits, natural levees, and floodplain deposits characterized by crevasse splays (Li, 2018a; North and Warwick, 2007). Channel deposits are predominantly composed of medium-to fine-grained sandstones (Figure 3a), with GR curves showing medium-to high-amplitude box-shaped or bell-shaped patterns. Floodplain deposits, mainly consisting of mudstones and siltstones, are dominated by crevasse splay microfacies and often exhibit horizontal laminations (Li, 2018a). Due to arid climatic conditions, intense evaporation cause most rivers and episodic floods to gradually disappear, fluvial fans facies are deposited above the lake shoreline without entering the lake (Donselaar et al., 2013; Li and Bristow, 2015; Tooth, 2000). According to statistical data, from the upstream (the Yanchi - Dingbian area in the northwest of the basin) to the downstream (the Tongchuan - Huanglong area in the southeast of the basin), the total length exceeds 300 km. As the slope decreases, the grain size of the sediment becomes finer, the thickness and width of the single sand body decrease, and the frequency of the occurrence of fans increases. Such river types and sedimentary microfacies characteristics are very similar to the large fluvial fan sedimentary system of the Chinle Formation in the Upper Triassic of Arizona (Trendell et al., 2013). The difference is that the end of the fluvial fan sedimentary system of the Chinle Formation was injected into the axial fluvial system, while the end of the meander fluvial system of the Yanchang Formation remains undetermined.

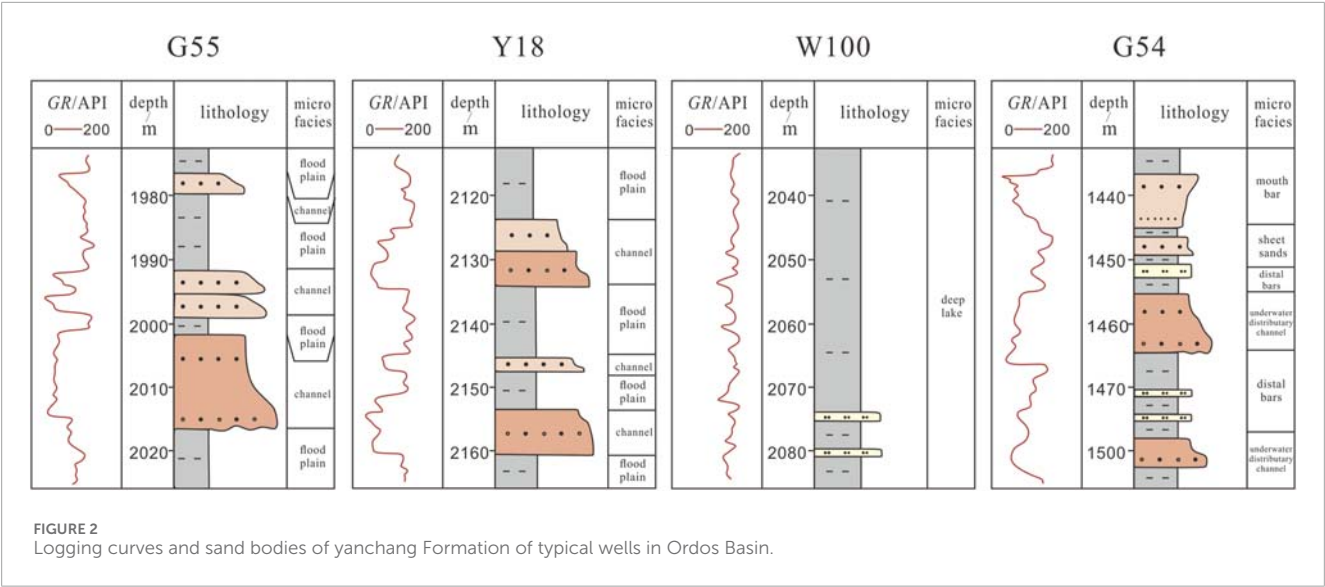
From the perspective of fluvial fan formation under arid conditions, arid environments and flooding events are key factors in their development. The repeated avulsion and migration of terrestrial rivers form amalgamated fluvial fans

TABLE 1 Types and characteristics of main sedimentary systems of Yanchang Formation.

Sedimentary facies type	Climate conditions	Location	Lithology	Sedimentary pattern	Transport mechanism	Plant coverage situation	Sedimentary structure	Hydrodynamic strength	Typical deposition unit
Fluvial fan	Arid and the annual precipitation is less than the annual evaporation	Open depressions adjacent to upland areas (Zhang et al., 2020a)	Mainly sandstone, (muddy) siltstone	Fan-shaped in plan, wedge-shaped in profile (Zhang et al., 2020b)	Traction flow dominated (Zhang et al., 2020c)	Rare	Dominated by massive stratification, granular stratification (Wang et al., 2023)	Strong-Medium (Wang et al., 2023)	Waste channel
Lacustrine	Dry or wet	Lakes and depressions (Song et al., 2009)	Mudstone and siltstone dominate	Circumferential band in the plane	Traction flow, gravity flow (Deng et al., 2009)	Prosperity	There are both structures reflecting traction currents, such as trough-like interbedded laminations, parallel laminations, etc., and sedimentary structures reflecting gravity currents. (Deng et al., 2009)	Weaker (Deng et al., 2009)	
Braidedriver delta	Humid and the annual precipitation is greater than the evaporation	Steeper boundaries of depression lake basins or slower boundaries of faulted lake basins (Wang et al., 2023)	Sandstone and conglomerate dominate	Mat-like in plan (Pu and Lu, 2000), lenticular in profile	Traction flow, sheet flow (Pu and Lu, 2000)	Prosperity	Large trough-like interbedded laminae, plate-like interbedded laminae, occasional estuarine dams, no sediment formed by tidal action	Comparatively strong (Yang et al., 2017)	Above/below water diversion channels
Meandering River delta	Humid and the annual precipitation is greater than the evaporation	On the transition zone of river and lake action with gentle drop and long slopes (Wang et al., 2023)	Sandstone and mudstone dominate (Wu et al., 2004)	Ornithopod-like or banded in plan (Wu et al., 2004), lenticular in profile	Traction flow dominated	Prosperity	Interbedded laminae, undulating interbedded laminae and scour-fill structures, common plant residual debris	Weaker (Yang et al., 2017)	Above/below water diversion channels

TABLE 2 Lithology and log characteristics of the main sedimentary system of Yanchang Formation.

Facies systems	subfacies	microfacies	Lithology	Logging facies	
				GR description of logging curve morphology	GR line graph
Fluvial fans	Diverging river channel		Sandstone is dominant, with conglomeratic sandstone, conglomerate, and discontinuous positive cyclicity features visible	Medium-High Box, Bell	 Y18 well 1190~1210m
	Floodplain		Fine sandstone, siltstone as the main	Low amplitude gearing linear	 Y18 well 1115~1125m
Lacustrine	Shallow lake		Siltstone; mudstone-siltstone	Low amplitude toothed line	 L148 well 1600~1615m
	Deep lake		Mudstone, siltstone	Extremely low amplitude microdentation line	 B420 well 2200~2215m
Delta	Delta plain	distributary channels	Sandstone-dominated, visible conglomerate-bearing sandstone and conglomerate, intermittent orthorhythmic features	Medium to high amplitude microtoothed bell or box shape	 Y52 well 2270~2290m
		natural levees	Fine sandstone and siltstone dominate	Medium-width toothed box shape	 Y52 well 2245~2260m
		interdistributary bays	Mudstone-dominated, interbedded grainy siltstone	Extremely low profile, linear	 Y75 well 1130~1140m
	Delta front	underwater distributary channels	Sandstone and siltstone dominate, orthorhythmic features	Medium-high amplitude microtoothed box or bell shape with mutant contact at bottom	 Y75 well 1515~1525m
		Underwater interdistributary bays	Mainly mudstone, a little siltstone, fine sandstone	Extremely low amplitude microdentation line	 Y75 well 1725~1735m
		mouth bars	Fine sandstone and siltstone dominate, anticlinal features	Medium-high amplitude microtoothed funnel-shaped	 Y75 well 1695~1710m
		distal bars	Dominated by siltstones, with minor mudstones and fine sandstones	Medium width toothed funnel shape	 Y75 well 1900~1920m
		sheet sands	Fine sandstone and siltstone dominate	Medium-High Smooth Finger	 Y75 well 1925~1935m
		Prodelta		Mudstone, silty mudstone, a few fine sandstones	Very low amplitude line shape



sandstone sheets, which can develop large-scale sand-rich reservoir facies (Zhang et al., 2020b).

4.1.2 Delta facies system

During the Yanchang Formation period, the Ordos Basin developed both meandering river deltas and braided river deltas (Deng et al., 2019; Guo et al., 2019; Li et al., 2024; Xu et al., 2023). Although slight differences in sedimentary characteristics exist due to variations in sediment transport distances caused by differing source proximities, these distinctions are not elaborated in detail in this study, and both types are collectively referred to as deltas.

Deltas are triangular sedimentary bodies formed when rivers transport sediments into seas or lakes, where the sediments are deposited due to flow diffusion and rapid velocity reduction in transitional environments between land and water. Based on lithology, logging curves, and other characteristics, deltas can be subdivided into three subfacies and a series of microfacies (Tables 1, 2). Delta facies are distributed throughout all periods of the Yanchang Formation, but their characteristics vary slightly under different tectonic and climatic conditions. During the arid early and late stages of the Yanchang Formation, delta deposits were primarily confined within the lake shoreline, with limited delta plain areas restricted by the shoreline. In contrast, during the humid middle stage of the Yanchang Formation, extensive delta deposits developed, no longer constrained by the lake shoreline.

(1) Delta Plain Subfacies

The delta plain subfacies, the subaerial part of deltaic deposits, mainly consists of sandstone, siltstone, and mudstone. In the study area, it includes distributary channels, interdistributary bays, and natural levees. Distributary channels are dominated by sandstone, showing coarsening-upward, discontinuous normal cycles (Figure 3c), with GR curves displaying medium-to high-amplitude serrated bell or box shapes. Interdistributary bays are primarily mudstone with laminated siltstone (Figure 3i), exhibiting very low-amplitude GR curves. Natural levees consist of medium-to fine-grained sandstone and siltstone (Figure 3b), with medium-amplitude serrated box-shaped GR curves.

(2) Delta Front Subfacies

The delta front subfacies, is the most active depositional zone and the main area for deltaic sand body development. It includes underwater distributary channels, interdistributary bays, mouth bars, distal bars, and sheet sands. Underwater distributary channels are dominated by sandstone and siltstone, showing fining-upward normal cycles and medium-to high-amplitude serrated box or bell GR curves (Figure 2). Interdistributary bays are mainly mudstone with minor siltstone and fine sandstone (Figure 3h), displaying mud-draped ripple cross laminations and very low-amplitude serrated GR curves. Mouth bars show medium-to high-amplitude serrated funnel-shaped GR curves (Figure 2), while distal bars exhibit medium-amplitude serrated funnel-shaped GR curves (Figure 2). Sheet sands are dominated by fine sandstone and siltstone (Figure 3j), with well-sorted, mature sandstone and medium-to high-amplitude smooth finger-shaped GR curves.

(3) Prodelta Subfacies

The prodelta subfacies, extending from the delta front into the lake, is mainly dark composed of mudstone and silty mudstone with minor fine sandstone. It commonly displays massive and horizontal bedding. As delta front sand bodies prograde, gravitational sliding or collapse can form turbidites in the prodelta.

4.1.3 Lacustrine facies system

This facies primarily develops in the central part of the basin and mainly includes subaqueous gravity flow deposits and semi-deep to deep lacustrine subfacies. The shore-shallow lacustrine subfacies is not discussed separately, as it is predominantly occupied by the delta front subfacies of braided and meandering rivers (Yang et al., 2017).

The semi-deep to deep lacustrine subfacies is dominated by lacustrine mud microfacies, with lithologies primarily consisting of argillaceous siltstone, black mudstone (Figures 3d–f), and oil shale. These deposits typically exhibit thick mudstone intervals interbedded with minor siltstone layers (Figure 2) and often display horizontal bedding, commonly alternated with turbidite deposits commonly observed within.

4.2 Sedimentary facies distribution and evolution

4.2.1 Sedimentary facies architecture

To reconstruct the sedimentary facies architecture in the study area, 15 representative wells were selected based on their facies systems assemblages, stratigraphic features, and spatial distribution. Two well-tied profiles were established: a SW–NE profile (Y52, Y22, L148, B420, X474, Y70, Y75, Y18) and a NW–SE profile (Y224, H254, Y196, X462, S214, W545, Q72).

(1) SW–NE Profile

The SW–NE profile (Figure 4A) is composed of braided river delta facies in the southwestern basin margin (i.e., wells Y52, Y22, L148) and of meandering river delta and fluvial fan systems in the northeast (wells, Y70, Y75, Y18), with semi-deep to deep lacustrine areas in the center of the profile (wells B420, X474). This profile is nearly parallel to the sediment source direction. During the early (Chang 10–Chang 8) and late (Chang 3–Chang 1) stages of the Yanchang Formation, sand bodies were widely distributed, with severe erosion observed in the Chang 1. From the Chang 9 depositional period, the semi-deep to deep lacustrine facies gradually transgressed, while deltaic sand bodies retreated. By the Chang 7 period, deep lacustrine facies were extensively developed, followed by a gradual reduction in lake area and the re-advancement of sand bodies. Vertically, the sequence reflects a large-scale cycle of lake-level rise and fall, indicating relatively stable water conditions.

(2) NW–SE Profile

The NW–SE profile (Figure 4B) is composed of braided river delta facies in the northwestern basin margin (i.e., wells Y224, H254) and of prodelta and delta front areas in the southeast (wells S214, W545, Q72), with semi-deep to deep lacustrine zones in the center of the profile (wells Y196, X462). This profile is nearly perpendicular to the sediment source direction. Compared to the SW–NE profile, the deep lacustrine facies are more widely distributed, but the vertical evolution patterns are consistent.

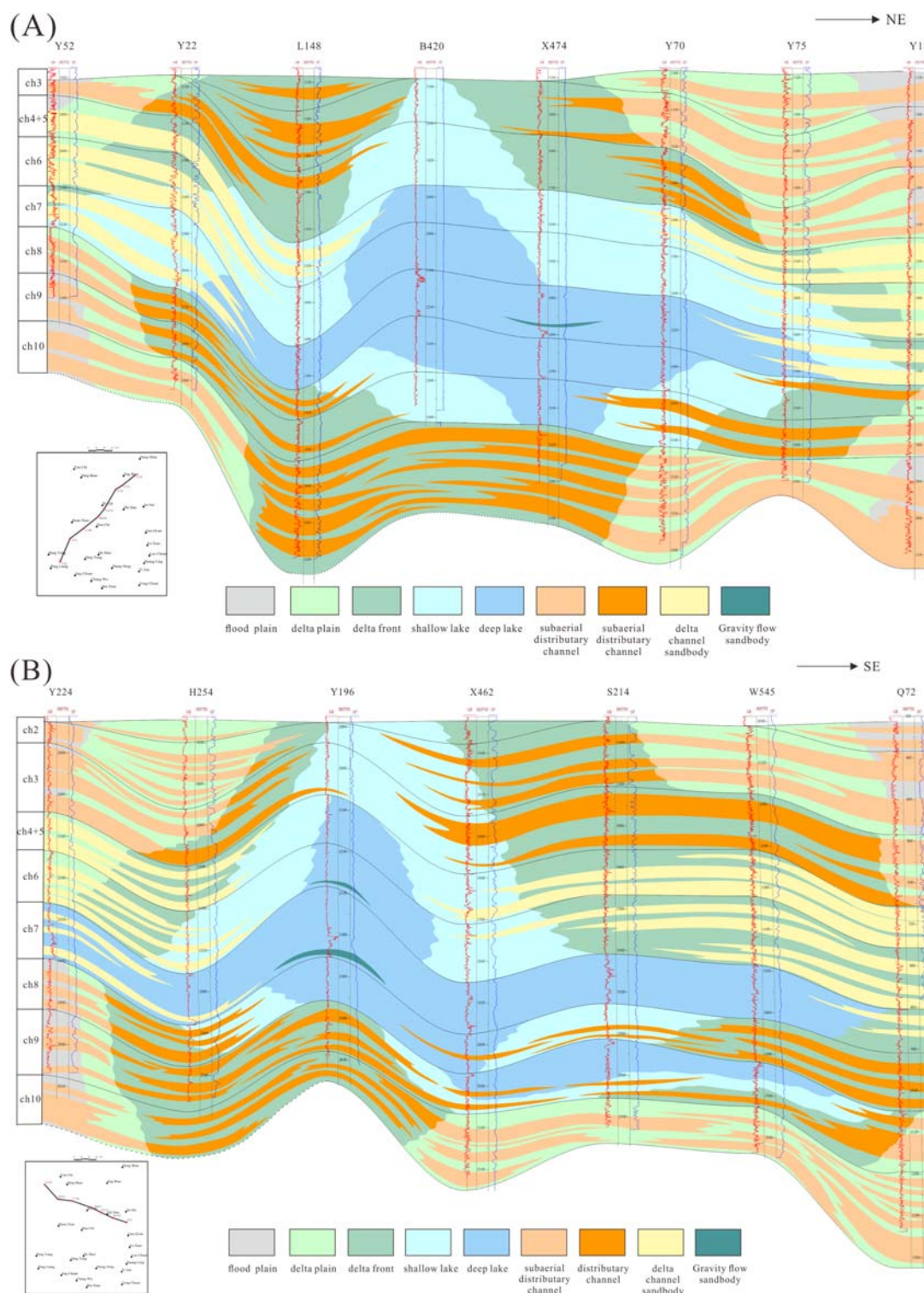
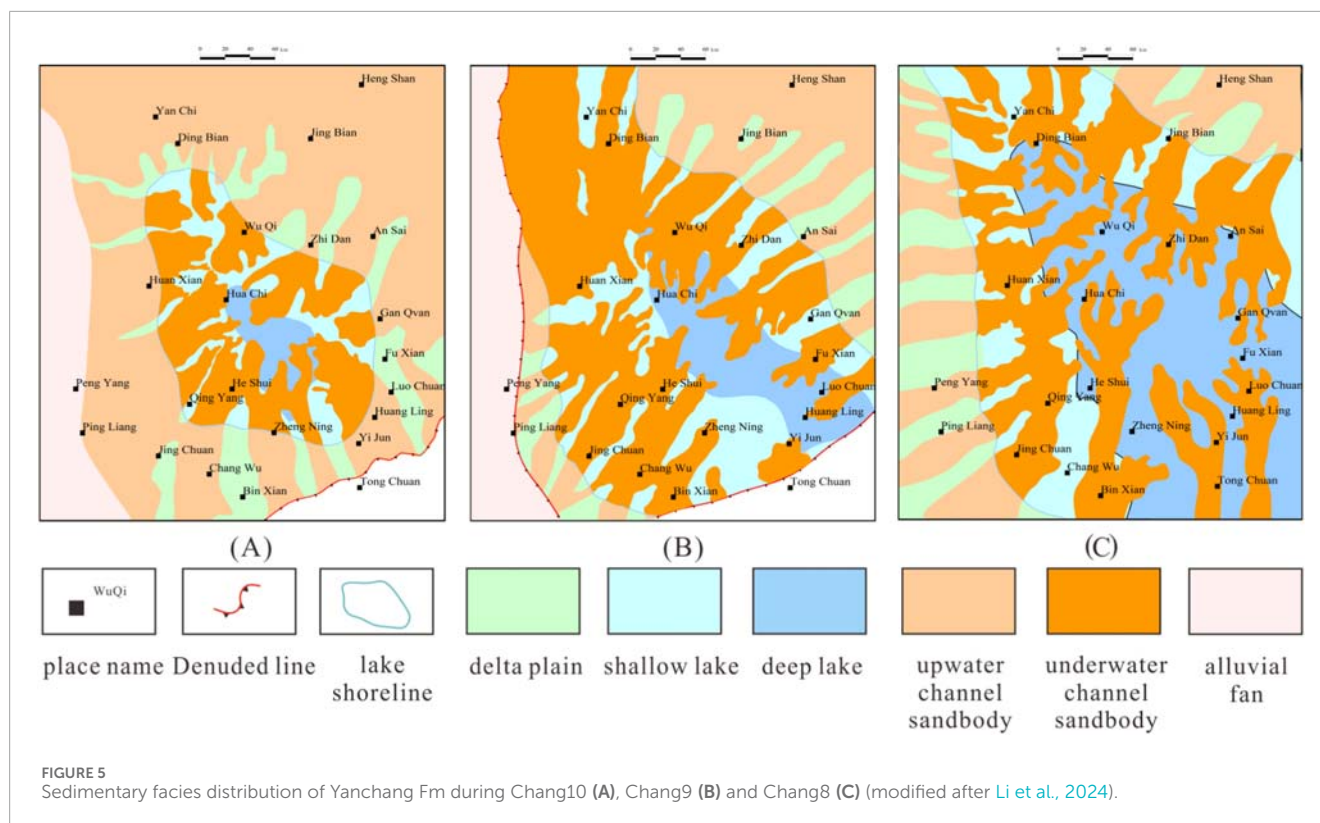


FIGURE 4
Typical connecting well profile of Yanchang Formation; (A) SW-NE; (B) NW-SE.

4.2.2 Areal distribution of the sedimentary facies

Based on the analysis of sedimentary facies from selected wells in the Yanchang Formation of the Ordos Basin, a sedimentary facies map for the different Chang 10 to Chang 1 periods was compiled (Figure 5).

Yanchang Formation has been divided into three sequence development stages, as revealed by high-resolution 3D seismic profiles. These stages correspond to the Ladinian (Chang 10 ~ Chang 8), Carnian (Chang 7 ~ Chang 4 + 5), and Norian-Rhaetian (Chang 3 and above) stages. The boundaries between these



sequences are marked by abrupt changes in sedimentary facies, controlled by global alternations of arid and humid climatic conditions (Li et al., 2023b).

This study focuses on the sedimentary facies characteristics of the early Chang 10, middle Chang 7, and late Chang 2, as they represent key intervals of the Yanchang Formation. Other intervals exhibit similar sedimentary facies patterns and are not described in detail.

(1) Early Stage of Yanchang Formation (Chang 10 ~ Chang 8)

During the early Yanchang Formation, the climate was arid. The Chang 10 is characterized by flood episodic deposits under arid conditions, with the overall sedimentary framework dominated by floodplain deposits formed by fluvial fan systems. Due to the distant sediment source and decreasing gradient, sediment grain size becomes finer, and the thickness and width of individual sand bodies decrease, while the frequency of crevasse splays increases. As a result, fluvial fan deposits developed in the western, northern, and eastern parts of the study area, forming an extensive floodplain depositional system where river channels terminated beyond the lake shoreline. The central region was primarily dominated by deltaic and lacustrine deposits. Meandering River Systems distributed in the northern and eastern parts of the basin, with microfacies including channels, swamps, point bars, floodplains, and natural levees. Braided River Systems located in the western and southwestern parts of the basin, with microfacies such as channel lag deposits, mid-channel bars, floodplains, and overbank deposits. Mid-channel bars are the most developed, often exhibiting large-scale trough cross-bedding formed by channel migration. The lacustrine area was relatively small, with the shoreline extending south of Dingbian, Wuqi, and Zhidan,

reaching as far south as Qingyang and Zhengning, and not extending beyond Huanxian to the west (Figure 5A).

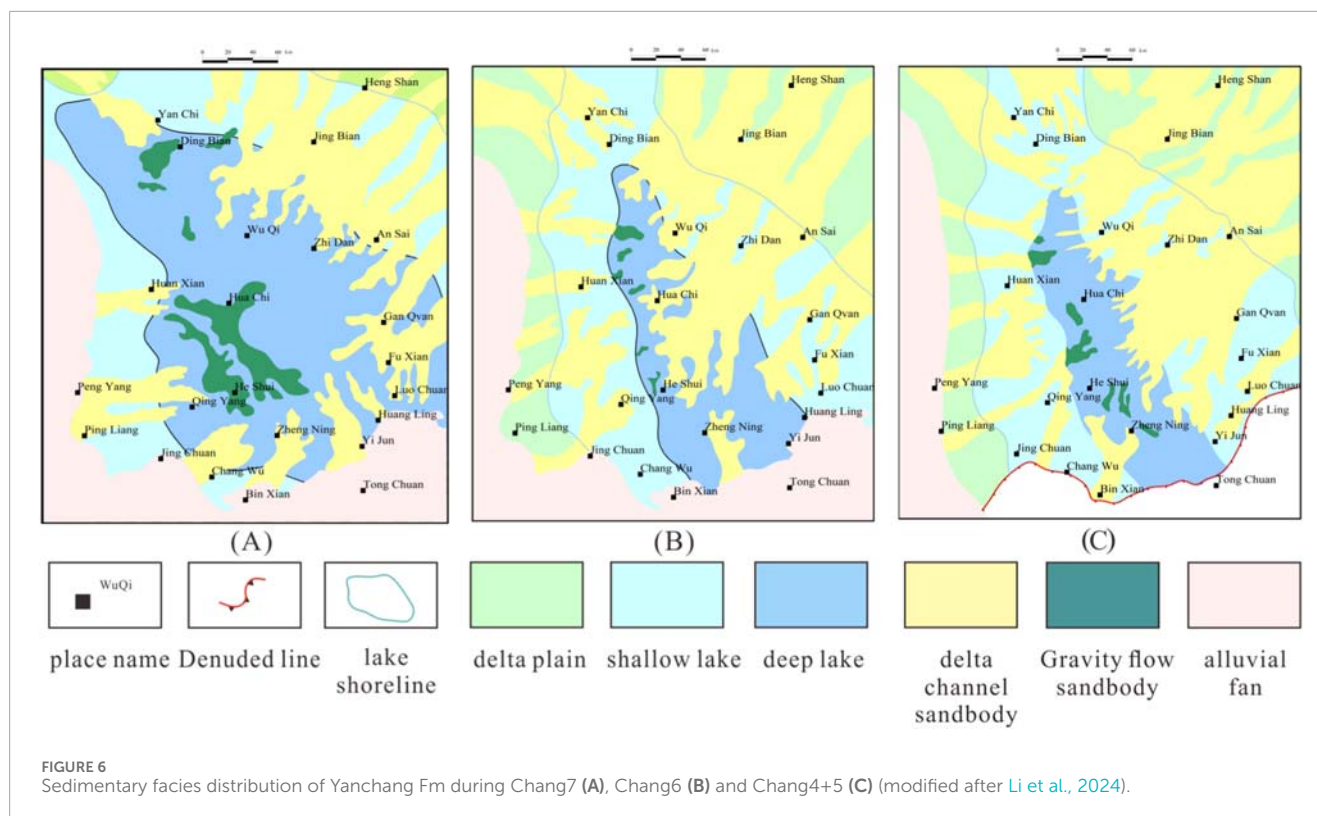
During the Chang 9 period, under arid conditions and influenced by tectonic activity, the lake basin expanded, and water levels rose, leading to a transgression. The lake area increased, and the shoreline extended to areas such as Yanchi, Jingbian, Ansai, Yan'an, and Huangling. Deltaic deposits became more developed during this period, with sand bodies predominantly surrounding the lake basin (Figure 5B).

In the Chang 8 period, the lake basin continued to expand, and the shoreline advanced further north to areas beyond Jingbian. The northern deltaic deposits expanded, while the fluvial fan deposits became less extensive. The braided river delta deposits in the southeastern margin showed little change in scale (Figure 5C).

(2) Middle Stage of Yanchang Formation (Chang 7 ~ Chang 4 + 5)

During the middle Yanchang Formation, the climate was humid. This period was characterized by abundant rainfall and a rapid increase in the catchment area. Abrupt climatic events led to significant changes in sedimentary facies, primarily dominated by deltaic deposits under humid conditions. The tectonic lake basin reached its maximum expansion, with the northern and eastern boundaries of shallow lake sediments extending to the Wuzhong–Prague–Uxin Banner line and the Hengshan east–Zichang–Yichuan east line, respectively.

A complete continental river-delta-lake-gravity flow sedimentary system developed. These deposits formed a fine-grained sedimentary system rich in organic matter, providing an excellent foundation for the development of shale oil in the Chang 7. Meandering river delta deposits were primarily developed in the



northern part of the basin, with minor delta front deposits in the southwest. Additionally, turbidite fans formed by gravity flows were present in the deep lake area. The delta-gravity flow complex system is a defining feature of this period in the study area (Figure 6A).

During the Chang 6 period, the climate remained humid. Under tectonic control, the lake basin contracted, and the lake area decreased, while deltaic deposits expanded further. The northern and eastern lake shorelines retreated to the Yanchi–Ansai–Yan'an line. In the western and southwestern parts of the basin, braided river delta front deposits expanded and formed contiguous sections. Meanwhile, meandering river delta deposits in the northeast advanced southward (Figure 6B).

In the Chang 4 + 5 period, the lake shoreline changed little. Both the braided river delta deposits in the southwest and the meandering river delta deposits in the northeast developed extensive delta plains (Figure 6C), with widespread overbank swamp mudstones.

(3) Late Stage of Yanchang Formation (Chang 3~Chang 1)

During the late Yanchang Formation, the climate transitioned to arid and semi-arid conditions. The basin experienced uplift due to tectonic activity, resulting in significant erosion on the basin margins.

In the Chang 3 stage, deep lacustrine deposits disappeared, and shallow lacustrine sediments significantly contracted, retreating southward to the Dingbian–Ansai–Yan'an line. Fluvial fan sedimentation accelerated in the north and advanced further south (Figure 7A).

The Chang 2 stage was characterized by arid conditions, with the basin dominated by fluvial fan sedimentary systems and extensive

floodplain development, similar to the early Yanchang Formation. Under tectonic influence, erosion intensified, and the shoreline further narrowed to the Wuqi–Zhidan line. Large-scale fluvial fan deposits developed in the north, while meandering river delta deposits were restricted to areas such as Huachi. Braided river delta deposits in the southwest were distributed in Zhengning, Heshui, and western Qingyang (Figure 7B).

During the Chang 1 stage, the basin experienced further erosion, but the distribution of the lake basin can be inferred through sedimentary facies analysis. At this stage, braided river delta deposits disappeared, leaving only meandering river delta deposits. The fluvial fan sedimentary system was distributed in the northern regions of Shenmu, Yulin, and Jingbian, as well as in Yan'an and Ganquan in the southeast. Shallow lacustrine sediments fragmented into several small lakes, distributed in the Dingbian area to the west, the Zichang–Ansai area to the east, and the Huachi and Zhengning areas to the southwest. Within the shallow lacustrine sediments of the Zichang area, small zones of deep lacustrine deposits were present, accompanied by turbidite fan deposits (Figure 7C).

5 Discussion

5.1 Age model for the studied Yanchang Formation

Based on the established biostratigraphic framework (Deng et al., 2018), significant differences in palynofloral assemblages were identified between the lower (Chang 10–Chang 8) and

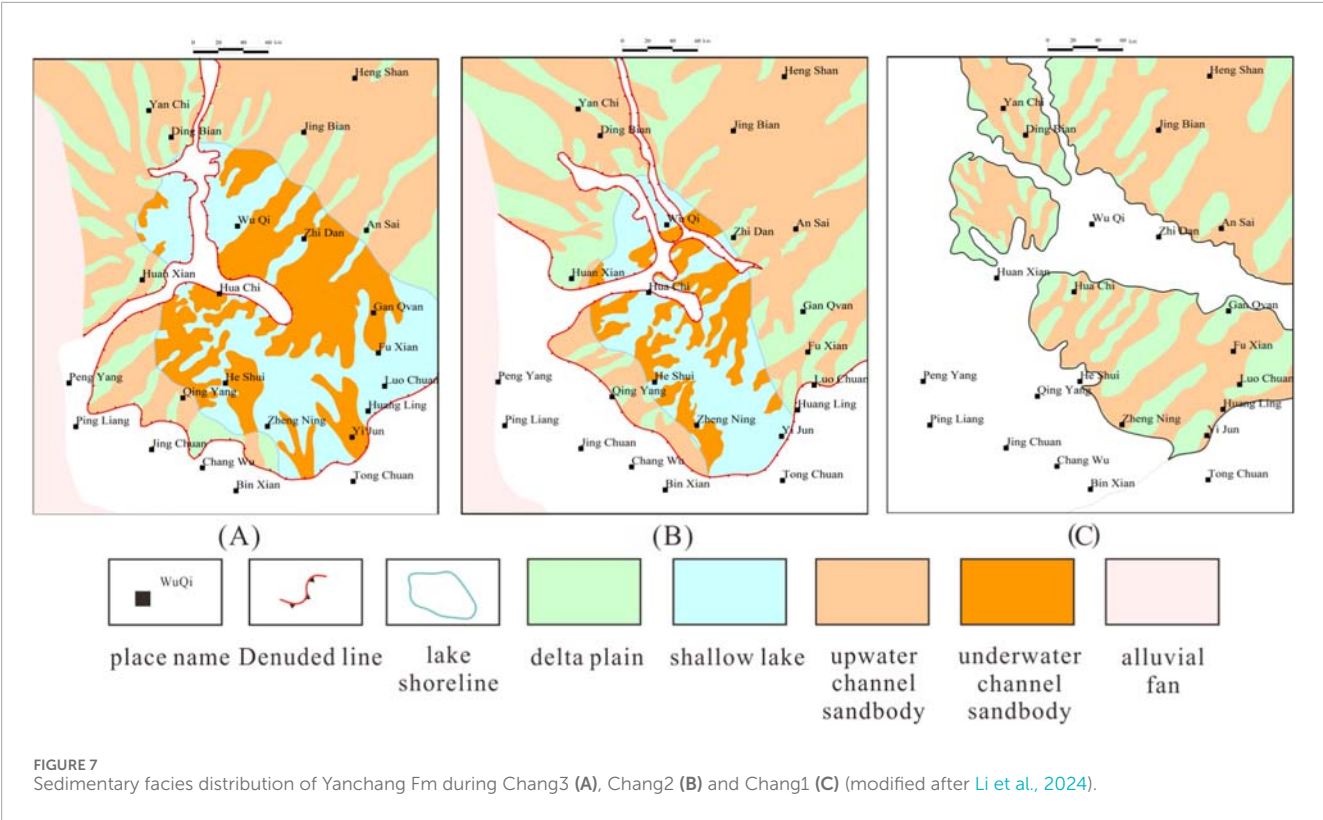


FIGURE 7 Sedimentary facies distribution of Yanchang Fm during Chang3 (A), Chang2 (B) and Chang1 (C) (modified after Li et al., 2024).

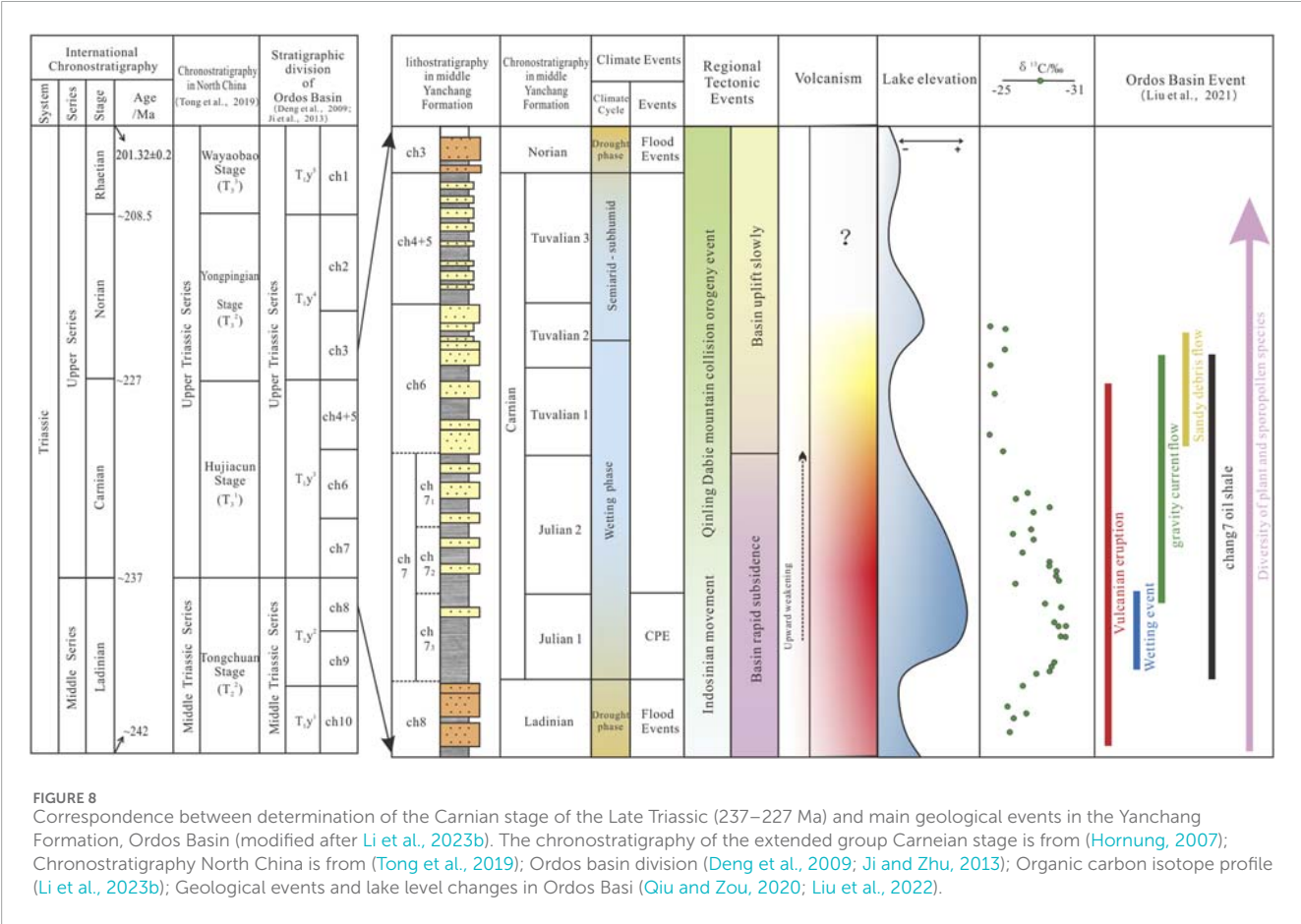
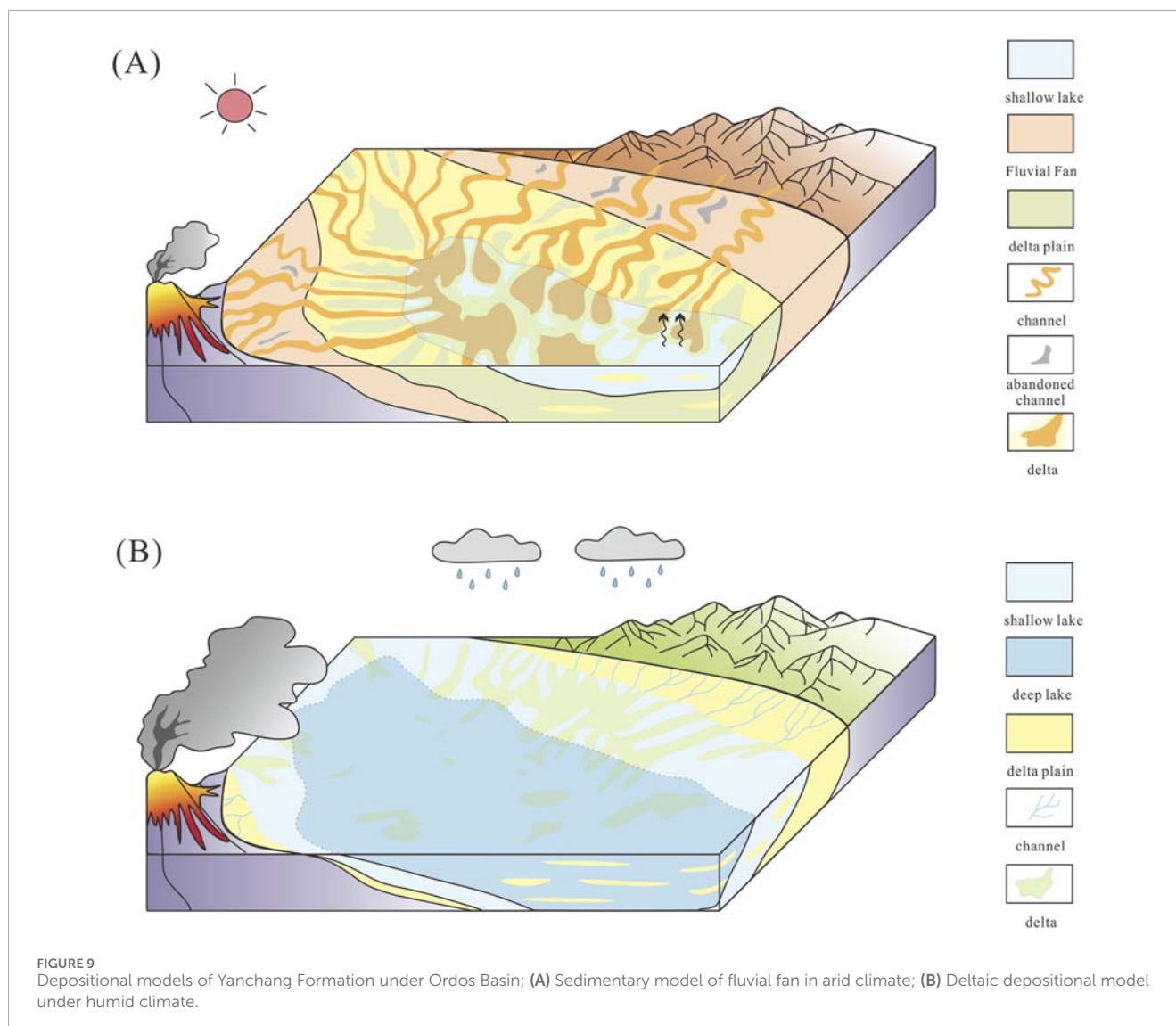


FIGURE 8 Correspondence between determination of the Carnian stage of the Late Triassic (237–227 Ma) and main geological events in the Yanchang Formation, Ordos Basin (modified after Li et al., 2023b). The chronostratigraphy of the extended group Carnian stage is from (Hornung, 2007); Chronostratigraphy North China is from (Tong et al., 2019); Ordos basin division (Deng et al., 2009; Ji and Zhu, 2013); Organic carbon isotope profile (Li et al., 2023b); Geological events and lake level changes in Ordos Basi (Qiu and Zou, 2020; Liu et al., 2022).



middle-upper (Chang 7–Chang 1) intervals of the Yanchang Formation, reflecting distinct climatic conditions. The lower interval is characterized by a *Punctatisporites*–*Aratrisporites*–*Verrucosisporites* assemblage, while the middle-upper interval contains an *Asseretospora*–*Apiculatisporis*–*Chordasporites* assemblage.

High-precision U–Pb dating of tuffaceous interbeds provides critical chronological constraints: Deng et al. (2013) obtained weighted mean ages of 221.8 ± 2.0 Ma and 228.2 ± 2.0 Ma from tuff layers in the upper and lower Chang 7 member, respectively, in two southern basin wells. Zhang et al. (2014) reported ages of 234–236 Ma from three southwestern wells. Wang et al. (2014) determined ages of 241.3 ± 2.4 Ma and 239.7 ± 1.7 Ma at the base of Chang 7 in two southwestern wells. Wang et al. (2017) obtained ages of 226.5 ± 1.6 Ma and 229.7 ± 2.2 Ma from tuffs at the base of Chang 7 in the Tongchuan area, with detrital zircon minimum age populations of 235–243 Ma. According to the International Chronostratigraphic Chart (2025), the Ladinian–Carnian boundary is dated at 237 Ma. These geochronological data suggest that the

base of the Chang 7 member likely corresponds to the Middle–Late Triassic boundary.

In this study, the method proposed by Tong Jinnan for dividing the Triassic strata in North China is adopted (Tong et al., 2019). Specifically, the lower boundary of the Carnian Stage in the Yanchang Formation is approximately equivalent to the stratigraphic boundary between the Chang 7 and Chang 8, while the upper boundary corresponds to the boundary between the Chang 4 + 5 and Chang 3.

5.2 Global and local factors controlling the deposition of Yanchang Formation

Based on this stratigraphic framework, the deposition of the Chang 7 period coincided with the global Carnian Pluvial Episode (CPE) event, a tentative correlation between the studied succession and the global CPE was possible. The CPE was a global climatic event, characterized by negative carbon isotope excursions and

anoxia, resulting in the deposition of black shales. This global event was accompanied by increased precipitation, rising temperatures, and intensified continental weathering (Jin et al., 2022; Miller et al., 2017; Mueller et al., 2016; Roghi et al., 2010; Zhao et al., 2019). During the early Chang 7, the sedimentary environment underwent abrupt changes, with significant lithological and facies variations observed near the Chang 7/Chang 8 boundary (Li et al., 2023b). Based on analyses of sedimentary environments and lithofacies, we propose that the Chang 7 black mudstone-shale series represents a product of the CPE event. In fact, Carnian organic-rich black shales were widely deposited in the northwestern Paleo-Tethys Ocean, Southern Alps, Iran, Himalayas, Indonesia, as well as South China and western Sichuan regions of China. These deposits are generally considered genetically linked to the CPE event and are commonly referred to as the “Carnian black shale event” (Dal Corso et al., 2012; Zhao et al., 2019).

The Chemical Index of Alteration (CIA) serves as an important geochemical indicator for revealing continental CPE records and has been applied to studies of Carnian lacustrine strata. CIA values in the Chang 8 member remain relatively low, fluctuating between 66.37–80.42 with an average of 72.43, while in the Chang 7 member they reach relatively higher values (Li et al., 2025). Moreover warm and humid climates favour the development of terrestrial vegetation which might result in negative carbon isotope excursion of the organic matter in sediments ($\delta^{13}\text{C}_{\text{org}}$), while in arid climates, are rather characterized by more positive $\delta^{13}\text{C}_{\text{org}}$ (Figure 8). In this regard negative excursions of the organic carbon isotope records have been observed (Dal Corso et al., 2012; Jin et al., 2015; Wang and Zhang, 1999; Zhao et al., 2019). Additionally, Li et al. (2023b) integrated paleoclimate, paleosol, geochemical data, and abrupt sedimentary facies changes to confirm that the Chang 7 to Chang 4 + 5 period represents a major transition interface between alternating dry and wet climates. Fu et al. (2018) further utilized ratios of rare earth and trace elements (e.g., Sr/Cu) to reflect paleoclimate aridity and humidity. This study has been proved that the climate and environment during the Chang 7 period was warm and humid. These line of evidences can reflect the climate fluctuation recorded in the studied Yanchang Formation; In particular (Li et al., 2023b) (Figure 8). The middle Yanchang Formation (Chang 7 ~ Chang 4 + 5) was warm and humid, while the early (Chang 10 ~ Chang 8) and late (Chang 3 ~ Chang 1) periods were relatively arid.

Climatic conditions significantly control terrigenous clastic deposition, and the CPE event triggered a series of responses in the long-term arid Triassic strata. First, the CPE event altered sediment transport and deposition patterns in the Yanchang Formation, increasing the input of terrigenous debris, leading to significant changes in continental sedimentary records before and after the event (Dal Corso et al., 2020; Jamaluddin et al., 2024). For example, The reduction of the Sr/Ba value indicate a transition from saline lake to freshwater lake sediments (Fu et al., 2018), accompanied by the widespread distribution of deltaic sediments and coal deposits (Kozur and Bachmann, 2010).

Although climate directly influences sedimentation, tectonic events also play a critical role. Tectonic factors were particularly significant during the extreme climatic events of the Carnian Stage. Mountain uplift caused by plate convergence introduced large amounts of detrital material, leading to distinct sedimentary responses. Concurrently, volcanic eruptions associated with the

closure of the Paleo-Tethys Ocean impacted climate, increasing precipitation (Jin et al., 2015).

During the Triassic Yanchang Formation, the stable tectonic background of the Ordos Basin may have minimized the influence of tectonic activity. However, tectonic events, including volcanic eruptions and abrupt climate changes, interacted with other factors to shape the depositional patterns of the Yanchang Formation (Qiu and Zou, 2020).

5.3 Sedimentary model

Based on the analysis of sedimentary facies evolution and controlling factors, sedimentary models for the Yanchang Formation under arid and humid paleoclimate conditions were established (Figure 9).

(1) Arid Paleoclimate Environment

Under arid conditions, the lake area was limited, and the primary sedimentary units included deltas, floodplains, and seasonal or abandoned channels with strong evaporation effects. Sandstone deposits were widely distributed, characterized by traction flow in channel sand bodies, forming a sedimentation model typical of fluvial fans (Figure 9A). The formation process can be summarized as follows: in a long-term arid environment, intense mechanical and physical weathering produced abundant fine-grained detrital material, which accumulated in and around the basin. During rainstorms, surface runoff or floods transported large amounts of sediment radially from the basin center. Due to evaporation, most flooding episodes occurred above the shoreline of the arid lake basin, depositing sediments near the lake shoreline. Frequent flood events and river avulsion eventually formed delta-like, fan-shaped sandy deposits in the lake basin center, resulting in the extensive sand-rich deposits of the Yanchang Formation in the Ordos Basin.

(2) Humid Paleoclimate Environment

Under humid conditions, the lake area expanded significantly, and a complete continental river-delta-lake-gravity flow sedimentary system developed, dominated by lake-delta-gravity flow sedimentation (Figure 9B). Stable, long-term flowing water fixed river channels, allowing sediments to be transported and deposited along these channels. This setting was highly beneficial to delta formation, with relatively stable lake-level changes.

5.4 Petroleum geological significance

Traditionally, the delta depositional system has been considered dominant in the Yanchang Formation, with limited explanation for the variations in sand body distribution. This study introduces the concept of a fluvial fan sedimentary system—a flood-dominated floodplain system under arid conditions (Zhang Y.F. et al., 2020). This system exhibits an alternating distribution of rivers and floodplains, forming a fan-shaped sedimentation model. This perspective enriches and refines the traditional understanding of sedimentation, suggesting that the large depression lake basin of the Yanchang Formation is not solely dominated by deltaic deposits. This advancement holds significant

implications for enhancing the theoretical framework of continental basin sedimentation and guiding oil and gas exploration practices.

Additionally, this study emphasizes the impact of major geological events, such as abrupt climatic changes, on the Ordos Basin, particularly their influence on sedimentary facies. The Carnian Pluvial Episode (CPE) and similar events created optimal conditions for the development of high-quality source rocks. First, during the CPE, increased precipitation caused rapid lake-level rise, while volcanic eruptions contributed to a reducing environment. Intermittent floods transported terrigenous detrital materials and nutrient-rich volcanic materials into the lake basin, promoting the proliferation of organisms such as algae (Qiu and Liu, 2014; Shi et al., 2010; Wang et al., 2023). Second, during the late CPE, as the paleoclimate shifted to arid and semi-arid conditions, the lake level exhibited “oscillating transgressive-regressive” patterns, characterized by alternating high and low levels (Li et al., 2021). This led to periodic dilution and concentration of lake water in a closed environment, further enhancing the development of high-quality source rocks.

During the CPE, the Yanchang Formation developed extensive high-quality source rocks (Li et al., 2023a) and large-scale delta-gravity flow reservoir sand bodies. In the preceding and subsequent arid periods, large-scale fluvial fan sand bodies formed above and below the source rocks, serving as excellent reservoir units. The fluvial fan sandstones in arid environments, combined with high-quality source rocks in humid environments, provide favorable conditions for hydrocarbon accumulation and significant exploration potential. However, frequent river avulsion during arid periods may result in poor sand body connectivity, necessitating improved exploration techniques.

In summary, the key factors controlling conventional and unconventional reservoir formation in the Yanchang Formation are closely linked to abrupt geological events. Qiu Zhen et al. extensively studied major Phanerozoic geological events and found that they significantly influence the distribution of oil and gas resources, particularly unconventional resources. Their work confirms that the sedimentary processes of key elements in hydrocarbon-rich areas are closely associated with global or regional geological events, whether in continental or marine basins (Guo et al., 2019; Pan et al., 2021; Qiu and Zou, 2020).

6 Conclusion

1. The Carnian Pluvial Episode (CPE) event has controlled sediment transport and deposition in the Yanchang Formation in the Ordos Basin. Although abrupt climate changes were the main factors controlling sedimentary characteristics, tectonic events and volcanic activity were also key drivers.
2. Sedimentary facies characteristics of the Yanchang Formation (from Chang1 to Chang10 periods) were analyzed using logging curves and lithology data. The facies architecture for each period were defined, and well-tied profiles and planar maps were constructed to establish a sedimentary facies evolution model for the entire Yanchang Formation under alternating dry and wet conditions. In arid paleoclimate

environments, fluvial fan sedimentary systems developed, while in humid environments, lake-delta-gravity flow systems dominated.

3. This study challenges the traditional view of the Yanchang Formation as a shallow-water delta environment formed under a humid climate. Instead, it identifies fluvial fan sedimentary systems during arid periods. The division of fluvial fan sedimentary facies enriches the theoretical understanding of continental basin sedimentation and guides oil and gas exploration. Fluvial fan sandstones in arid environments, combined with high-quality source rocks from humid periods, create favorable conditions for hydrocarbon accumulation and offer significant exploration potential.

Data availability statement

The original contributions presented in the study are included in the article/supplementary material, further inquiries can be directed to the corresponding author.

Author contributions

YF: Conceptualization, Data curation, Investigation, Methodology, Writing – original draft, Writing – review and editing. LJ: Funding acquisition, Investigation, Project administration, Writing – review and editing. HJ: Conceptualization, Methodology, Writing – review and editing. YG: Conceptualization, Supervision, Writing – review and editing. WZ: Project administration, Supervision, Writing – review and editing. TZ: Writing – review and editing. YH: Data curation, Investigation, Writing – review and editing.

Funding

The author(s) declare that financial support was received for the research and/or publication of this article. This work is supported by CNPC Scientific Research and Technology Development Project “Whole petroleum system theory and unconventional hydrocarbon accumulation mechanism” (2021DJ0101).

Conflict of interest

The authors declare that the research was conducted in the absence of any commercial or financial relationships that could be construed as a potential conflict of interest.

Generative AI statement

The author(s) declare that no Generative AI was used in the creation of this manuscript.

Publisher's note

All claims expressed in this article are solely those of the authors and do not necessarily represent those of their affiliated

organizations, or those of the publisher, the editors and the reviewers. Any product that may be evaluated in this article, or claim that may be made by its manufacturer, is not guaranteed or endorsed by the publisher.

References

- Cain, S. A., and Mountney, N. P. (2009). Spatial and temporal evolution of a terminal fluvial fan system: the Permian organ rock formation, south-east Utah, USA. *Sedimentology* 56 (6), 1774–1800. doi:10.1111/j.1365-3091.2009.01057.x
- Carroll, A., Graham, S., and Smith, M. (2010). Walled sedimentary basins of China. *Basin Res.* 22 (1), 17–32. doi:10.1111/j.1365-2117.2009.00458.x
- Dal Corso, J., Mietto, P., Newton, R. J., Pancost, R. D., Preto, N., Roghi, G., et al. (2012). Discovery of a major negative $\delta^{13}\text{C}$ spike in the Carnian (late Triassic) linked to the eruption of wrangellia flood basalts. *Geology* 40 (1), 79–82. doi:10.1130/g32473.1
- Dal Corso, J., Bernardi, M., Sun, Y., Song, H., Seyfullah, L. J., Preto, N., et al. (2020). Extinction and dawn of the modern world in the Carnian (late Triassic). *Sci. Adv.* 6 (38), eaba0099. doi:10.1126/sciadv.aba0099
- Deng, X. Q., Lin, F. X., Liu, X. Y., Pang, J. L., Lv, J. W., and Li, S. X. (2008). Discussion on relationship between sedimentary evolution of the Triassic Yanchang Formation and the Early Indosinian Movement in Ordos Basin. *J. Palaeogeogr.* 10 (02), 159–166.
- Deng, X. Q., Li, W. H., Liu, X. S., Pang, J. L., and Liu, X. (2009). Discussion on stratigraphic boundary between Middle Triassic and Upper Triassic in Ordos Basin. *Acta Geol. Sin.* 83 (08), 1089–1096.
- Deng, X. Q., Luo, A. X., Zhang, Z. Y., and Liu, X. (2013). Geochronological comparison on Indosinian tectonic events between Qinling orogeny and Ordos Basin. *Acta Sedimentol. Sin.* 31 (6), 939–953.
- Deng, S. H., Lu, Y. Z., Luo, Z., Ru, F., Li, X., and Zhao, Y. (2018). The division, age and middle-Upper Triassic boundary of Yanchang Formation in Ordos Basin. *Sci. China Earth Sci.* 48 (10), 1293–1311.
- Deng, X. Q., Zhang, W. X., Li, W. H., Sun, B., Zhou, X. P., and Cheng, D. X. (2019). The relationship between middle-Upper Triassic sedimentary filling characteristics and low grade petroleum system of Yanchang Formation in Ordos Basin. *J. Northwest Univ. Nat. Sci. Ed.* 49 (04), 622–632.
- Deng, X. Q., Chu, M. J., Wang, L., Chen, X., and Wang, Y. (2024). Two stages of Ordos Basin subsidence and its formation mechanism in the Middle and Late Triassic. *Petroleum Explor. Dev.* 51 (03), 501–512.
- Donselaar, M., Gozalo, M. C., and Moyano, S. (2013). Avulsion processes at the terminus of low-gradient semi-arid fluvial systems: lessons from the río Colorado, Altiplano endorheic basin, Bolivia. *Sediment. Geol.* 283, 1–14. doi:10.1016/j.sedgeo.2012.10.007
- Fu, J. H., Guo, Z. Q., and Deng, X. Q. (2005). Sedimentary facies and petroleum geological significance of the Upper Triassic Yanchang Formation in southwest Ordos Basin. *J. Palaeogeogr.* (01), 34–44.
- Fu, J. H., Li, S. X., Xu, L. M., and Niu, X. B. (2018). Restoration and significance of paleosedimentary environment of Chang 7 Member of Yanchang Triassic in Ordos Basin. *Petroleum Explor. Dev.* 45 (06), 936–946.
- Galloway, W. E., Hobday, D. K., Galloway, W. E., and Hobday, D. K. (1996). “Terrigenous clastic depositional systems: applications to fossil fuel and groundwater resources,” in *Terrigenous shelf systems*, 159–185. doi:10.1007/978-3-642-61018-9_7
- Gao, Y., Jiang, L., Chen, W., Dong, H., Jiang, F., Zhao, W., et al. (2025). Tectonic evolution of the proto-paleo-tethys in the west kunlun orogenic belt: constraints from U-Pb geochronology of detrital zircons. *Gondwana Res.* 141, 213–227. doi:10.1016/j.gr.2025.02.010
- Guo, Y. Q., Li, W. H., Guo, B. C., Zhang, Q., Chen, Q., and Wang, R. G. (2019). Sedimentary system and paleogeographic evolution of Ordos Basin. *J. Palaeogeogr.* 21 (02), 293–320.
- Hartley, A. J., Weissmann, G. S., Nichols, G. J., and Warwick, G. L. (2010). Large distributive fluvial systems: characteristics, distribution, and controls on development. *J. Sediment. Res.* 80 (2), 167–183. doi:10.2110/jsr.2010.016
- Hornung, T. (2007). Multistratigraphy of the draxllehen quarry near berchtesgaden (Tuvallian-lacian 2): implications for hallstatt lime-stone-sedimentation and paleoclimate in aftermath of the carnian crisis. *Austrian J. Earth Sci.* 100.
- Hu, Y., Jia, C.-Z., Chen, J.-Q., Pang, X.-Q., Jiang, L., Wang, C.-X., et al. (2025). Restoration of hydrocarbon generation potential of the highly mature Lower Cambrian yuertusi formation source rocks in the tarim basin. *Petroleum Sci.* 22 (2), 588–606. doi:10.1016/j.petsci.2024.12.001
- Jamaluddin, K., Schöpfer, K., Wagreich, M., Gier, S., and Fathy, D. (2024). Effect of depositional environment and climate on organic matter enrichment in sediments of the upper miocene—pliocene kampungbaru formation, lower kutai basin, Indonesia. *Geosciences* 14 (6), 164. doi:10.3390/geosciences14060164
- Ji, L. M., and Zhu, Y. H. (2013). “Palynological association and paleoclimate of Yanchang Formation in Xifeng area of Gansu Province, southwest Ordos Basin,” in *Palynological association and paleoclimate of Yanchang Formation in Xifeng area of Gansu Province, southwest Ordos Basin* 30 (04), 367–378.
- Jin, X., Shi, Z. Q., Wang, Y. Y., Duan, X., and Cheng, M. (2015). Extreme climate events in the Middle Carnian period of the Late Triassic: research progress and problems. *Acta Sedimentol.* 33 (01), 105–115. doi:10.14027/j.cnki.cjxb.2015.01.011
- Jin, X., Franceschi, M., Martini, R., Shi, Z. Q., Gianolla, P., Rigo, M., et al. (2022). Eustatic sea-level fall and global fluctuations in carbonate production during the Carnian pluvial episode. *Earth Planet. Sci. Lett.* 594, 117698. doi:10.1016/j.epsl.2022.117698
- Kozur, H. W., and Bachmann, G. (2010). The middle Carnian wet intermezzo of the stuttgart formation schilfsandstein, Germanic basin. *Palaeogeogr. Palaeoclimatol. Palaeoecol.* 290 (1-4), 107–119. doi:10.1016/j.palaeo.2009.11.004
- Li, J. G. (2018a). Fine-grained sedimentary system and sedimentary model at the end of meandering river in arid lake basin. *Earth Sci.* 43 (S1), 264–276.
- Li, J. G. (2018b). Sedimentary model of fine-grained dryland meandering river terminus systems in a semi-arid or arid endorheic basin. *Earth Sci.* 43 (S1), 264–276.
- Li, J. G., and Bristow, C. S. (2015). Crevasse splay morphodynamics in a dryland river terminus: río Colorado in Salar de Uyuni Bolivia. *Quat. Int.* 377, 71–82. doi:10.1016/j.quaint.2014.11.066
- Li, W. H., Liu, X., Zhang, Q., Guo, Y. Q., Li, K. Y., and Yuan, Z. (2019). Middle and late Triassic Yanchang sedimentary evolution in Ordos Basin. *J. Northwest Univ. Nat. Sci. Ed.* 49 (04), 605–621. doi:10.16152/j.cnki.xdxbr.2019-04-013
- Li, X. B., Liu, H. Q., Deng, X. Q., Wang, Y. T., Long, L. W., and Wei, L. H. (2021). The concept of river fan in arid environment and new explanation of genesis of “full basin sand” in Yanchang Formation of Ordos Basin. *Acta Sedimentol.* 39 (05), 1208–1221. doi:10.14027/j.issn.1000-0550.2020.077
- Li, X. B., Liu, H. Q., Huang, J. P., Wang, Y. T., Hao, B., and Long, L. W. (2023a). Wet-dry climate alternations and the formation and distribution of fan sand bodies in inland lacustrine basins: A case study of Yanchang Formation, Ordos Basin. *Acta Geol. Sin.* 97 (03), 822–838. doi:10.19762/j.cnki.dizhixuebao.2021271
- Li, X. B., Liu, H. Q., Yang, W. W., Zhang, Y., Zavala, C., and Ji, L. M. (2023b). An inland lake basin dominated by alternating wet-dry extreme climatic events: sedimentological evidence from the outcrop profile of the Upper Triassic Yanchang Formation in the Ordos Basin. *Earth Sci.* 48 (01), 293–316.
- Li, X. B., Zhu, R. K., Hui, X., Su, M. J., Qiu, Z., and Huang, J. P. (2023c). Sedimentological response of Late Triassic Carnian Meiyu Event (CPE) in continental basin: a case study of Yanchang Formation, Ordos Basin. *Acta Sedimentol.* 41 (02), 511–526. doi:10.14027/j.issn.1000-0550.2022.008
- Li, W. H., Zhang, Q., Li, Z. Y., Li, K. Y., Guo, Y. Q., and Feng, J. P. (2024). Lithofacies paleogeography and sedimentary evolution of Ordos Basin and its periphery. *J. Northwest Univ. Nat. Sci. Ed.* 54 (06), 929–949. doi:10.16152/j.cnki.xdxbr.2024-06-001
- Li, J. G., Wei, Y., Yang, B., and Lei, X. T. (2025). Response of Kani Period rain curtain events in the southern Ordos Basin area. *Acta Geol. Sin.* 99 (02), 365–381. doi:10.19762/j.cnki.dizhixuebao.2023330
- Liu, H. Q., Yvan, J. Y., Li, X. B., Wan, Y. R., and Liao, J. B. (2007). “Evolution and genetic analysis of lacustrine basin in ordos basin during yanchang period,” in *Lithologic Reservoir* (01), 52–56.
- Liu, H. Q., Li, X. B., Wan, Y. R., Wei, L. H., and Liao, J. B. (2011). Paleogeographic environment and sedimentary characteristics of Chang8 oil formation in Ordos Basin. *Acta Sedimentol.* 29 (06), 1086–1095. doi:10.14027/j.cnki.cjxb.2011.06.005
- Liu, Q. Y., Li, P., and Jin, Z. J. (2022). Organic matter rich formation and hydrocarbon enrichment in lacustrine shale strata: a case study of chang 7. *Sci. China Earth Sci.* 52 (02), 270–290. doi:10.1007/s11430-021-9819-y
- Lu, X. X., Li, M. L., and Wang, W. (2008). Indosinian movement and Indosinian mineralization in Qinling Orogenic belt. *Depos. Geol.* 27 (06), 762–773.
- Lu, Q. Q., Fu, J. H., and Luo, S. S. (2022). Sedimentary characteristics and models of gravity channel-lobe complex in a depression lacustrine basin: a case study of chang 7 member of yanchang Triassic in southwest ordos basin. *Petroleum Explor. Dev.* 49 (06), 1143–1156.
- Miller, C. S., Peterse, F., Da Silva, A. C., Baranyi, V., Reichart, G. J., and Kürschner, W. M. (2017). Astronomical age constraints and extinction mechanisms of the Late Triassic Carnian crisis. *Sci. Rep.* 7 (1), 2557. doi:10.1038/s41598-017-02817-7

- Mueller, S., Krystyn, L., and Kürschner, W. M. (2016). Climate variability during the Carnian pluvial phase—A quantitative palynological study of the Carnian sedimentary succession at lunz am see, northern calcareous alps, Austria. *Palaeogeogr. Palaeoclimatol. Palaeoecol.* 441, 198–211. doi:10.1016/j.palaeo.2015.06.008
- Nakada, R., Ogawa, K., Suzuki, N., Takahashi, S., and Takahashi, Y. (2014). Late Triassic compositional changes of aeolian dusts in the pelagic panthalassa: response to the Continental climatic change. *Palaeogeogr. Palaeoclimatol. Palaeoecol.* 393, 61–75. doi:10.1016/j.palaeo.2013.10.014
- Nichols, G. J., and Hirst, J. P. (1998). Alluvial fans and fluvial distributary systems, oligo-miocene, northern Spain; contrasting processes and products. *J. Sediment. Res.* 68 (5), 879–889. doi:10.2110/jstr.68.879
- North, C. P., and Warwick, G. L. (2007). Fluvial fans: myths, misconceptions, and the end of the terminal-fan model. *J. Sediment. Res.* 77 (9), 693–701. doi:10.2110/jstr.2007.072
- Pan, S. X., Wei, P. S., Wang, T. Q., Wang, J. G., Liang, S. J., Zhao, Z. K., et al. (2012). Sedimentary characteristics of flood-overlake in large depression basin taking the 4th member, quantou formation, Lower Cretaceous, in southern songliao basin as an example. *Geol. Rev.* 58 (1), 41–52.
- Pan, S. Q., Zou, C. N., Li, Y., Jing, Z. H., Liu, E. T., and Yvan, M. (2021). Major biological events and the formation and evolution of fossil energy: on the development of energy science under the framework of Earth system. *Petroleum Explor. Dev.* 48 (03), 498–509.
- Pang, J. G., Chang, L. J., and Guo, J. A. (2022). Lacustrine channel-lobe turbidite fan sedimentary model of Yanchang Formation in southern Ordos Basin. *J. Northwest Univ. Nat. Sci. Ed.* 52 (01), 144–158. doi:10.16152/j.cnki.xdxzbzr.2022-01-016
- Parrish, J. T. (1993). Climate of the supercontinent pangea. *J. Geol.* 101 (2), 215–233. doi:10.1086/648217
- Parrish, J. T., and Peterson, F. (1988). Wind directions predicted from global circulation models and wind directions determined from eolian sandstones of the Western united states—A comparison. *Sediment. Geol.* 56 (1-4), 261–282. doi:10.1016/0037-0738(88)90056-5
- Pu, T., and Lu, Z. Y. (2000). Characteristics, reservoir properties and classification of lake braided river deltas. *Sediment. Tethian Geol.* (01), 78–84.
- Qiu, X. W., and Liu, C. Y. (2014). Filling types and development of high-quality source rocks in the Yanchang lacustrine basin of Ordos Basin. *Acta Geol. Sin.* 35 (01), 101–110.
- Qiu, Z., and Zou, C. N. (2020). Unconventional oil and gas sedimentology: connotation and prospect. *Acta Sedimentol.* 38 (01), 1–29. doi:10.14027/j.issn.1000-0550.2019.116
- Roghi, G., Gianolla, P., Minarelli, L., Pilati, C., and Preto, N. (2010). Palynological correlation of Carnian humid pulses throughout Western tethys. *Palaeogeogr. Palaeoclimatol. Palaeoecol.* 290 (1-4), 89–106. doi:10.1016/j.palaeo.2009.11.006
- Schlager, W., and Schöllnberger, W. (1974). Das Prinzip stratigraphischer Wenden in der Schichtfolge der Nördlichen Kalkalpen. *Mitt. Geol. Ges. Wien* 66 (67), 165–193.
- Shi, Z. Q., Qian, L. J., Xiong, Z. J., and Zeng, D. Y. (2010). Discussion on the crisis and its causes in the Carnian period in southwest China. *Bull. Mineralogy, Petrology Geochem.* 29 (03), 227–232.
- Simms, M. J., and Ruffell, A. H. (1989). Synchronicity of climatic change and extinctions in the Late Triassic. *Geology* 17 (3), 265–268. doi:10.1130/0091-7613(1989)017<0265:soccae>2.3.co;2
- Song, F., Hou, J. G., Zhang, Z., and Su, N. N. (2009). The microfacies of continental lake deposition was studied by using logging curves. *Logging Technology* 33 (06), 589–592.
- Stanistreet, I. G., and McCarthy, T. (1993). The okavango fan and the classification of subaerial fan systems. *Sediment. Geol.* 85 (1-4), 115–133. doi:10.1016/0037-0738(93)90078-j
- Tong, J. N., Chu, D. L., Liang, L., Shu, W. C., Song, H. J., and Song, T. (2019). Triassic comprehensive stratigraphy and time frame in China. *Sci. China Earth Sci.* 49 (01), 194–226.
- Tooth, S. (2000). Process, form and change in dryland Rivers: a review of recent research. *Earth-Science Rev.* 51 (1-4), 67–107. doi:10.1016/s0012-8252(00)00014-3
- Trendell, A. M., Atchley, S. C., and Nordt, L. C. (2013). Facies analysis of a probable large-fluvial-fan depositional system: the Upper Triassic chinle formation at petrified forest national park, Arizona, USA. *J. Sediment. Res.* 83 (10), 873–895. doi:10.2110/jstr.2013.55
- Tusken, J., Li, J. H., and Li, W. B. (2014). Triassic global plate reconstruction and lithofacies paleogeography. *Mar. Geol. Quat. Geol.* 34 (5), 153–162.
- Wang, D. Y., Xin, B. S., Yang, H., Fu, J. H., and Yao, J. L. (2014). Zircon SHRIMP U-Pb age and geological implications of tuff at the bottom of Chang-7 Member of Yanchang Formation in the Ordos Basin. *Sci. China Earth Sci.* 57 (12), 2966–2977.
- Wang, J. Q., Liu, C. Y., Li, X., Wu, T. T., and Wu, J. L. (2017). Geochronology, potential source and regional implications of tuff intervals in Chang-7 Member of Yanchang Formation, South of Ordos Basin. *Acta Sedimentol. Sin.* 35 (4), 691–704.
- Wang, S. M., and Zhang, Z. K. (1999). New progress in the study of lake deposition and environmental evolution in China. *Sci. Bull.* (06), 579–587.
- Wang, L., Li, W. H., Liu, Q., Wang, D. X., Zhang, M. B., and Bai, B. (2023). Lithofacies classification and depositional environment restoration of Black shale in chang 7, yanchang, ordos basin. *J. Palaeogeogr.* 25 (03), 598–613.
- Weissmann, G., Hartley, A., Nichols, G., Scuderi, L., Olson, M., Buehler, H., et al. (2010). Fluvial form in modern Continental sedimentary basins: distributive fluvial systems. *Geology* 38 (1), 39–42. doi:10.1130/g30242.1
- Wu, F. L., Li, W. H., Li, Y. H., and Xi, S. L. (2004). Delta sedimentation and evolution of Yanchang Formation of Upper Triassic in Ordos Basin. *J. Palaeogeogr.* (03), 307–315.
- Xie, F. Q., Xiao, W. Z., Sami, M., Sanislav, I. V., Ahmed, M. S., Zhang, C. G., et al. (2024). Tectonic evolution of the northeastern paleo-tethys ocean during the Late Triassic: insights from depositional environment and provenance of the xujiahe formation. *Front. Earth Sci.* 12, 1444679. doi:10.3389/feart.2024.1444679
- Xu, M. H., Wang, F., Chun, J., Ren, Z. C., Meng, H., and Yv, W. (2023). Lithofacies division and sedimentary environment of lacustrine organic-rich mudshale: a case study of chang 73 submember in ordos basin. *Acta sedimentol.*, 1–24.
- Yang, H., Liang, X. W., and Niu, X. B. (2017). Geological conditions of continental tight oil formation and main controlling factors of enrichment: a case study of Member 7 of Triassic Yanchang Formation, Ordos Basin. *Petroleum Explor. Dev.* 44 (01), 12–20.
- Zavala, C., and Freije, R. H. (2001). On the understanding of aeolian sequence stratigraphy: an example from Miocene-Pliocene deposits in patagonia, Argentina. *Riv. Ital. Paleontol. Stratigr.* 107 (2). doi:10.54103/2039-4942/16129
- Zhang, Y. P., Chen, X. H., Zhang, J., Shao, Z. G., Ding, W. C., and Guo, X. G. (2019). Discussion on the initiation time of the Indochinese movement in the ordos and sichuan basins: evidence from growth strata. *Geol. China* 46 (05), 1021–1038.
- Zhang, H., Peng, P. A., and Zhang, W. Z. (2014). Zircon U-Pb ages and Hf isotope characterization and their geological significance of Chang 7 tuff of Yanchang Formation in Ordos Basin. *Acta Petrol. Sin.* 30 (2), 565–575.
- Zhang, C. M., Wang, X. L., Chen, Z., Wu, T., Xiang, H., and Zhao, K. (2020a). Sedimentary characteristics of ephemeral and intermittent channels: a case study of the baiyanghe fan, Xinjiang, China. *Earth Sci.* 45 (05), 1791–1806.
- Zhang, C. M., Zhu, R., Guo, X., Wang, X., Yin, T., and Yuan, R. (2020b). Arid fluvial fandelta-fluvial fan transition: implications of huangyangquan fan area. *Earth Sci.* 45 (5), 1791–1806.
- Zhang, Y. F., Dai, X., Wang, M., and Li, X. X. (2020c). The concept, characteristics and significance of river fan. *Petroleum Explor. Dev.* 47 (05), 947–957.
- Zhang, R., Jin, Z. J., Li, M. S., and Liu, Q. Y. (2023). Astronomical control of organic-rich shale development in the Middle Triassic ordos basin. *Quat. Res.* 43 (06), 1547–1561.
- Zhao, X. D., Xue, N. H., Wang, B., and Zhang, H. C. (2019). Advances in the study of wet-curtain events of the Triassic carneian period. *J. Stratigr.* 43 (03), 306–314.